Near-*K*-edge single and double photoionization of C^{2+} ions

A. Müller,[1,*] A. Borovik, Jr.,[1] K. Holste,[1] S. Klumpp,[2] M. Martins,[3] and S. Schippers[1]

[1]*I. Physikalisches Institut, Justus-Liebig-Universität Gießen, 35392 Giessen, Germany*

[2]*DESY Photon Science, 22607 Hamburg, Germany*

[3]*Institut für Experimentalphysik, Universität Hamburg, 22761 Hamburg, Germany*

(Received 17 December 2022; accepted 16 February 2023; published 7 March 2023)

Single and double ionization of berylliumlike C^{2+} by a single photon is investigated in the energy range from 292 to 350 eV in the vicinity of the *K*-shell single-ionization threshold. Energy resolutions range between 160 meV for overview scans and 11 meV for high-resolution spectroscopy. The experimental cross sections include contributions from the $1s^22s^2\ {}^1S$ ground level and the $1s^22s2p\ {}^3P$ metastable levels. A comparison of the experimentally derived cross-section function for photoabsorption by C^{2+} to a model based on previous *R*-matrix calculations shows very satisfying agreement.

DOI: 10.1103/PhysRevA.107.032806

I. INTRODUCTION

Carbon is one of the most abundant heavy elements in the universe [1]. It is ubiquitous in astrophysical environments. Moreover, it is the prime constituent of organic chemistry and the building block of life on Earth. In both collisionally ionized and photoionized astrophysical gases, carbon atoms occur singly or multiply charged, and the ions can serve as probes for the state of the environment in which they are formed [2]. Important diagnostic techniques rely on soft-x-ray spectroscopy of carbon atoms and ions or carbon-containing molecules, especially near the *K* edge. This is particularly relevant for understanding the structure and dynamics of small organic as well as complex biological molecules [3].

Photoionization near the *K* edge of carbon ions was studied previously for C^+ [4–6], C^{2+} [7], C^{3+} [8], C^{4+} [9], and C^- [10–12]. Aspects of deep-core photoexcitation of ions were reviewed several years ago [13]. Valence-shell photoionization of C^{2+} ions has also been studied [14,15]. With the exception of the latest experiments on C^+ [5,6] and C^- [12], all other measurements were restricted to one ionization channel (mostly single ionization) of the investigated ion. In the first experiments on C^- [10,11] only one single resonance feature was observed in the double-detachment channel. All experimental data published so far on *K*-shell-involving photoionization of positive ions, C^{2+}, C^{3+}, and C^{4+}, have been restricted to the few strongest $1s \rightarrow np$ ($n = 2, 3$) resonance features.

Here we report absolute cross-section measurements for single and double photoionization of C^{2+} in the energy range from 292 to 350 eV covering all single-excitation resonances below and several double-excitation features above the *K* edge. The experiments were performed at the photon-ion merged-beam setup PIPE (photon-ion spectrometer at PETRA III) [16,17] using monochromatized undulator radiation from the PETRA III synchrotron light source in Hamburg. PIPE is a permanent end station of soft-x-ray beamline P04 [18]. At energy-resolving powers reaching up to about 27 000 it was possible to measure the natural line shapes of the most prominent resonances and to determine the natural linewidths of core-excited singlet-*P* levels. The present data were used to infer the photoabsorption cross section of C^{2+}, which we compare to theoretical results obtained with advanced *R*-matrix calculations [2].

This presentation is structured as follows. Following this introduction, a brief overview of the experimental technique is provided together with details specific to the present measurements. The relativistic Hartree-Fock method used to calculate cross sections for direct *K*-shell ionization is explained. The experimental results are shown in detail. Contributions to the measured spectra arising from excitations of $C^{2+}(1s^22s^2\ {}^1S)$ ground-level ions and $C^{2+}(1s^22s2p\ {}^3P)$ excited metastable ions are disentangled on the basis of the previously published *R*-matrix calculations [2]. Lorentzian widths of the strongest photoabsorption lines are derived from the measurements. The paper ends with a summary.

II. EXPERIMENT

The experimental arrangement and procedures were described in detail previously [16,17]. In short, C^{2+} ions were produced in an electron-cyclotron-resonance ion source. The ions were accelerated to an energy of 12 keV, magnetically analyzed to obtain an isotopically pure beam which was then transported to the interaction region, collimated, and merged with the photon beam available at beamline P04 [18] of PETRA III. The product ions were separated from the parent ion beam by a dipole magnet inside which the primary beam was collected in a large Faraday cup. The photoionized ions were passed through a spherical 180° out-of-plane deflector to suppress background from stray electrons, photons, and ions and then entered a single-particle detector with nearly 100% detection efficiency. The high brightness and flux of the photon

*alfred.mueller@iamp.physik.uni-giessen.de

beam (2.3×10^{10} s^{-1} at 294 eV energy and 11 meV bandwidth) permitted tight collimation of the ion beam (30 nA).

The photon flux was measured with a calibrated photodiode. The photon energy scale was calibrated with an uncertainty of less than ±40 meV relative to known (lower-energy) photoionization resonances in C^{2+} [7]. At higher energies up to 350 eV, deviations of 70 meV may be possible due to the extrapolation of the energy axis applied. Doppler shifts due to the ion velocity directed opposite to the incoming photons were corrected for, with the correction factor of the laboratory photon energy being approximately 1.0015.

The ion yields obtained in the present experiments were corrected for the separately measured background and normalized to the absolute cross-section data obtained previously [7]. A complication is introduced by the fact that beams of berylliumlike ions inevitably comprise ions in metastable $1s^22s2p\ ^3P$ states in addition to $1s^22s^2\ ^1S$ ground-state ions [15]. By comparing measured data with state-of-the-art theoretical calculations one can determine the relative fractions of metastable and ground-level ions in the ion beam used for the measurements. Comparing the present results with the calculations for C^{2+} ions performed by Hasoğlu *et al.* [2] results in fractions $f_{\rm gs} = 0.68 \pm 0.1$ for ground-level ions and $f_{\rm ms} = 1 - f_{\rm gs}$ for the metastable component. These findings are compatible with the fractions inferred by Scully *et al.* [7]. They also fall into the range of typical fractions of metastable $1s^22s2p\ ^3P$ Be-like ions extracted from electron-cyclotron-resonance ion sources [15].

The resulting systematic total uncertainties of the absolute cross sections thus obtained are quite large and reach the ±50% level for the metastable ions. For the ground state the estimated uncertainty level is no less than ±30%. However, the comparison of theoretical predictions and experimental results for K-shell photoionization of atoms and ions collected during the last few decades has proven the high reliability of the theoretical calculations. The uncertainty of calculated cross sections for direct ionization of the K shell by a single photon can be estimated to be less than ±20%. Comparison of the present cross-section data with the prediction by Verner *et al.* [19] for direct K-shell ionization shows very good agreement. Thus, the uncertainty of the present results can be safely assumed to be at the ±20% level.

III. HFR CALCULATIONS

The cross sections for direct K-shell photoionization of the $C^{2+}(1s^22s^2\ ^1S)$ and $C^{2+}(1s^22s2p\ ^3P_J)$ $(J = 0, 1, 2)$ parent-ion states were modeled by *ab initio* configuration-interaction (CI) calculations on the basis of the Hartree-Fock method with relativistic extensions (HFR) applying the Cowan code [20]. The theoretical approach was described in detail previously [21].

For the description of the C^{2+} initial states, the CI expansion was chosen to include the bound configurations given in the second and fourth columns of Table I in addition to the initial configurations $1s^22s^2$ and $1s^22s2p$, respectively.

The direct photo single-ionization cross sections for the removal of a $1s$ electron were calculated from the dipole matrix elements $\langle\Psi_{\epsilon\ell}|er|\Psi(^1S_0)\rangle$ for the $^1S_0$ initial level and $\langle\Psi_{\epsilon\ell}|er|\Psi(^3P_{0,1,2})\rangle$ for the $^3P_{0,1,2}$ initial levels. The wave function $\Psi_{\epsilon\ell}$ represents the residual C^{3+} ion and the ionized electron with kinetic energy ϵ and angular momentum $\ell = s, p, d, f$ as given in the third and fifth columns of Table I, respectively. Due to the different couplings of angular momenta and electron spins in the residual ion, this results in several different ionization thresholds corresponding to the different possible LS terms of the core-excited C^{3+} ion.

TABLE I. Sets of interacting configurations (**A**, **B**, **C**) used to describe the initial levels $1s^22s^2\ ^1S_0$ (ground level) and $1s^22s2p\ ^3P_{0,1,2}$ (metastable levels) and their direct K-shell photoionization. **A** stands for the initial configurations, **B** stands for the additional bound configurations, and **C** stands for the continuum configurations considered together with the corresponding initial configurations. The third and fifth column characterize the associated ejected electron with its kinetic energy ϵ and angular momentum $\ell = s, p, d, f$.

	Core configuration	Free electron	Core configuration	Free electron
A	$1s^22s^2$		$1s^22s2p$	
B	$1s^22s2p$		$1s^22s^2$	
	$1s^22p^2$		$1s^22p^2$	
	$1s2s^22p$		$1s2s2p^2$	
	$1s2s^23p$		$1s2s2p3p$	
	$1s2s^24p$		$1s2s2p4p$	
	$1s2s^25p$		$1s2s2p5p$	
	$1s2s^26p$		$1s2s2p6p$	
	$1s2p^3$			
	$1s2p^23p$		$1s2s^23s$	
	$1s2s2p3s$		$1s2p^23s$	
C	$1s^22p$	$\epsilon(s,d)$	$1s2s^2$	$\epsilon(s,d)$
	$1s2s2p$	$\epsilon(s,d)$	$1s2p^2$	$\epsilon(s,d)$
	$1s^23p$	$\epsilon(s,d)$	$1s^22s$	$\epsilon(s,d)$
	$1s^24p$	$\epsilon(s,d)$	$1s^23s$	$\epsilon(s,d)$
	$1s^25p$	$\epsilon(s,d)$	$1s^22p$	$\epsilon(p,f)$
	$1s^26p$	$\epsilon(s,d)$	$1s2s2p$	$\epsilon(p,f)$
	$1s2s^2$	$\epsilon(p,f)$	$1s2p3s$	$\epsilon(p,f)$
	$1s2s3s$	$\epsilon(p,f)$	$1s^23p$	$\epsilon(p,f)$
	$1s2p^2$	$\epsilon(p,f)$	$1s^24p$	$\epsilon(p,f)$
	$1s^22s$	$\epsilon(p,f)$	$1s^25p$	$\epsilon(p,f)$
	$1s^23s$	$\epsilon(p,f)$	$1s^26p$	$\epsilon(p,f)$

The configurations added to the CI expansion for describing the $1s^{-1}$ core-excited states are included in Table I.

IV. RESULTS

A. Overview of resonant and direct ionization

Figure 1 provides an overview of the investigated cross sections for single and double ionization of the C^{2+} ion by a single photon. The spectra were measured at a constant width of 2000 μm of the monochromator exit slit. This resulted in an energy bandwidth of 160 meV at 294 eV. With a fixed exit slit the resolution is expected to increase with the square root of the photon energy; that is, it is about 175 meV at 350 eV.

Net single ionization or, in other words, the production of C^{3+} from C^{2+}, is dominated by resonance contributions, i.e., by two-step processes involving K-shell excitation and subsequent Auger decay. There is no sign of the K-shell ionization

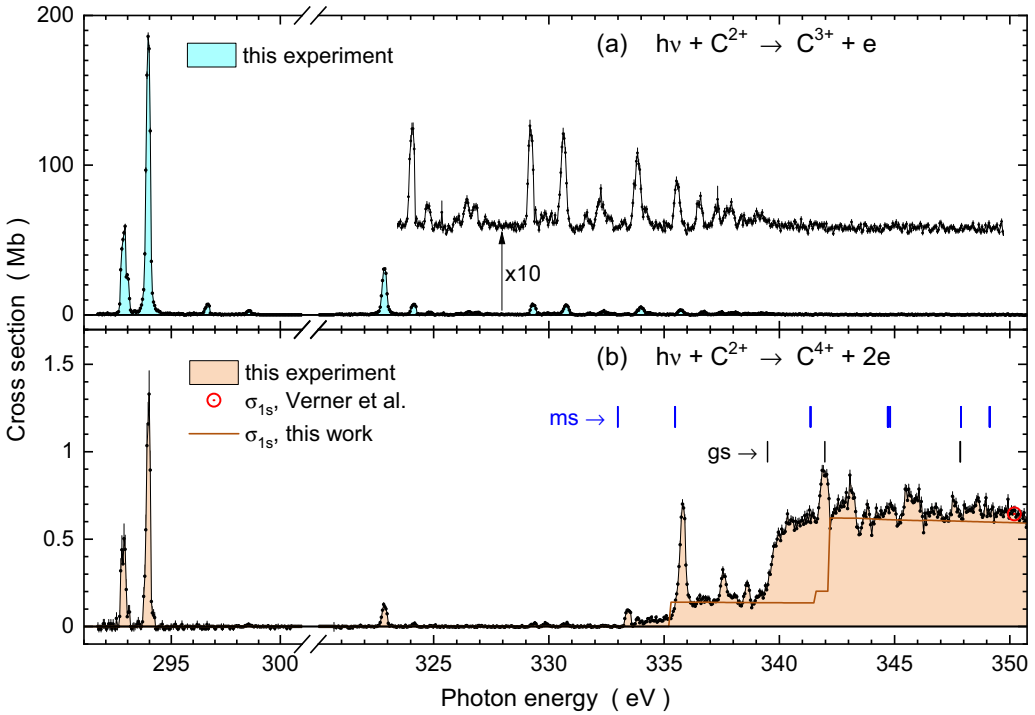

FIG. 1. Overview of the cross sections for photoionization of C^{2+} ions obtained in the present investigation with an energy resolution of 160 meV at 294 eV. The experimental cross-section functions for single-photon (a) single ionization and (b) double ionization are shown. Statistical uncertainties are displayed by vertical bars but are almost invisible. The strengths of resonance contributions to single ionization rapidly drop with increasing photon energy. For better visualization of the high-energy region, the measured cross sections were multiplied by a factor of 10 and displayed again with an offset. The open red circle shows the cross section for direct K-shell ionization at 350 eV calculated by Verner *et al.* [19]. The present HFR calculation of cross sections for direct K-shell single photoionization is represented by the solid brown line. The lower vertical black bars show calculated threshold energies for initial ground-state ions. The upper vertical blue bars show calculated threshold energies for initial metastable ions. For details see the text and Tables II and III.

onset in the measured cross section for net single ionization. This is straightforwardly explained for ground-level C^{2+} ions. The energetically lowest configuration populated by K-shell ionization of berylliumlike C^{2+} is $1s2s^2$. The most likely decays of the resulting $^2S_{1/2}$ level in lithiumlike C^{3+} were calculated by Goryaev *et al.* [22]. From their results a branching ratio for radiative decay of 1.9×10^{-4} can be inferred, leaving a probability of 99.98% for an Auger decay subsequent to direct K-shell ionization. The situation with metastable $C^{2+}(1s^22s2p\ ^3P)$ parent ions is more complex, with difficulties in assessing the decays of metastable $1s2s2p\ ^4P$ ions intermediately produced in the experiment.

Net triple ionization of the berylliumlike C^{2+} ion, i.e., the production of C^{5+}, is impossible in the investigated energy range since it would require a minimum energy of 504.47 eV for the ground state and at least 497.97 eV for the $1s^22s2p\ ^3P$ metastable levels [23]. Double-Auger decay of an intermediate $1s2sn\ell$ level is not possible because there are not enough electrons in the L shell for this process to happen. As a result, direct K-shell ionization predominantly contributes to the cross section for net double ionization, i.e., the production of C^{4+}, as shown in Fig. 1(b).

Along with the present experimental cross sections for net double ionization of C^{2+}, Fig. 1(b) displays theoretical results for direct K-shell photoionization of C^{2+} calculated by applying the present HFR method. For comparison, the plot also shows the result of a calculation by Verner *et al.* [19] at a photon energy of 350 eV. While the model used by Verner *et al.* is only for the ground configuration, the present HFR calculation additionally accounts for the initial metastable excited levels. To simulate the experimental conditions, a weighted sum of 68% ground-level contributions and 32% metastable-term contributions was chosen to obtain the solid brown line in Fig. 1.

Neither of the theoretical approaches considers the (indirect) contributions of K-shell excitation resonances to the observed net ionization cross sections. As discussed above, a single K vacancy in the intermediate C^{3+} ion decays with a high probability by single-Auger decay and thus predominantly contributes to net double ionization of the parent C^{2+} ion. The agreement of the present experiment with the theoretical predictions is quite satisfying at energies beyond about 345 eV, where resonance contributions become small. Resonances at energies beyond the K edge can occur only when at least two electrons are excited by a single photon, which is a process that occurs with a relatively low probability.

With the help of the NIST Atomic Spectra Database [23] and the precision calculations of $1s2\ell2\ell'$ energy levels in C^{3+} ions by Yerokhin *et al.* [24,25] the most important threshold energies for direct K-shell ionization of C^{2+} ions in the ground level or the metastable levels can be constructed by assuming hypothetical reaction chains leading to the desired C^{3+} core-hole level. An example is the onset of direct-ionization $1s^22s2p \rightarrow 1s2s^2$. In order to obtain the required photon

TABLE II. The lowest K-shell ionization thresholds (edge energies; in eV) of C^{2+} ions initially residing in their ground level [see the black vertical bars in Fig. 1(b)]. The intermediate excited $1s2\ell2\ell'$ levels are reached by the removal of a $1s$ electron from the $1s^22s^2\ {}^1S_0$ ground level. The number in parentheses in the third column is the uncertainty of the last digit, which is mainly determined by the contribution (see text) calculated by Yerokhin *et al.* [24,25].

Initial level	Intermediate level	Energy
$1s^22s^2\ {}^1S_0$	$1s2s^2\ {}^2S_{1/2}$	339.485(8)
	$1s[2s2p\ {}^3P]\ {}^4P_{1/2}$	341.976(2)
	$1s[2s2p\ {}^3P]\ {}^4P_{3/2}$	341.977(2)
	$1s[2s2p\ {}^3P]\ {}^2P_{1/2}$	347.845(2)
	$1s[2s2p\ {}^3P]\ {}^2P_{3/2}$	347.858(2)
	$1s[2p^2\ {}^3P]\ {}^4P_{1/2}$	351.195(2)
	$1s[2p^2\ {}^3P]\ {}^4P_{3/2}$	351.204(2)
	$1s[2p^2\ {}^3P]\ {}^4P_{5/2}$	351.210(2)
	$1s[2s2p\ {}^1P]\ {}^2P_{3/2}$	351.305(6)
	$1s[2s2p\ {}^1P]\ {}^2P_{1/2}$	351.306(6)
	$1s[2p^2\ {}^1D]\ {}^2D_{5/2}$	354.372(5)
	$1s[2p^2\ {}^1D]\ {}^2D_{3/2}$	354.385(5)
	$1s[2p^2\ {}^3P]\ {}^2P_{1/2}$	355.616(2)
	$1s[2p^2\ {}^3P]\ {}^2P_{3/2}$	355.635(2)
	$1s[2p^2\ {}^1S]\ {}^2S_{1/2}$	360.508(11)

TABLE III. The lowest K-shell ionization thresholds (edge energies; in eV) of C^{2+} ions in their $1s^22s2p$ metastable levels [see the blue vertical bars in Fig. 1(b)]. The intermediate excited $1s2\ell2\ell'$ levels are reached by the removal of a $1s$ electron from the $1s^22s2p\ {}^3P_{0,1,2}$ metastable levels. The threshold energies for the three metastable levels with total angular momentum quantum numbers J are provided in the columns labeled "Energy (J)". The numbers in parentheses represent the uncertainties of the last digits, which are mainly determined by the contributions (see main text) calculated by Yerokhin *et al.* [24,25].

Intermediate level	Energy ($J=0$)	Energy ($J=1$)	Energy ($J=2$)
$1s2s^2\ {}^2S_{1/2}$	332.992(8)	332.989(8)	332.982(8)
$1s[2s2p\ {}^3P]\ {}^4P_{1/2}$	335.484(2)	335.481(2)	335.474(2)
$1s[2s2p\ {}^3P]\ {}^4P_{3/2}$	335.484(2)	335.481(2)	335.474(2)
$1s[2s2p\ {}^3P]\ {}^2P_{1/2}$	341.353(2)	341.350(2)	341.343(2)
$1s[2s2p\ {}^3P]\ {}^2P_{3/2}$	341.365(2)	341.362(2)	341.355(2)
$1s[2p^2\ {}^3P]\ {}^4P_{1/2}$	344.702(2)	344.699(2)	344.692(2)
$1s[2p^2\ {}^3P]\ {}^4P_{3/2}$	344.712(2)	344.709(2)	344.702(2)
$1s[2p^2\ {}^3P]\ {}^4P_{5/2}$	344.717(2)	344.714(2)	344.707(2)
$1s[2s2p\ {}^1P]\ {}^2P_{3/2}$	344.812(6)	344.809(6)	344.802(6)
$1s[2s2p\ {}^1P]\ {}^2P_{1/2}$	344.813(6)	344.810(6)	344.803(6)
$1s[2p^2\ {}^1D]\ {}^2D_{5/2}$	347.879(5)	347.876(5)	347.869(5)
$1s[2p^2\ {}^1D]\ {}^2D_{3/2}$	347.892(5)	347.889(5)	347.882(5)
$1s[2p^2\ {}^3P]\ {}^2P_{1/2}$	349.124(2)	349.121(2)	349.114(2)
$1s[2p^2\ {}^3P]\ {}^2P_{3/2}$	349.142(2)	349.139(2)	349.132(2)
$1s[2p^2\ {}^1S]\ {}^2S_{1/2}$	354.015(11)	354.012(11)	354.005(11)

energy for the associated step in the cross-section function the following hypothetical chain of reactions can be considered in which the energies of the individual reactions are known with high accuracy from the sources cited above: $1s^22s2p \rightarrow 1s^22s^2 \rightarrow 1s^22s \rightarrow 1s^22p \rightarrow 1s2s^2$. Each configuration supports a certain number of levels so that multiple pathways may lead from the initial to the final level. Energies associated with one such pathway are −6.49269 eV (the relaxation energy of the $1s^22s2p\ {}^3P_0$ metastable level [23]), 47.88778 eV (the ionization threshold of the ground-state C^{2+} ion [23]), 7.99500 eV (the $1s^22s\ {}^2S_{1/2} \rightarrow 1s^22p\ {}^2P_{1/2}$ excitation energy of the ground-state C^{3+} ion [23]), and 283.60183(778) eV (the $1s^22p\ {}^2P_{1/2} \rightarrow 1s2s^2\ {}^2S_{1/2}$ transition energy in the C^{3+} ion [25]), where the uncertainty of the latter is in the last three digits given by the numbers in parentheses; that is, it is approximately 8 meV (rounded to the next highest third decimal). The sum of these energies is 332.992 ± 0.008 eV. It is shown as the first entry of the second column in Table III.

All individual pathways to the different direct-ionization thresholds with configurations $1s2s^2$, $1s2s2p$, and $1s2p^2$ are considered whenever accurate transition energies are available from the work of Yerokhin *et al.* [24,25]. The resulting energies are provided in Table II for ground-state C^{2+} ions and in Table III for metastable C^{2+} ions. The K-shell ionization energies below 351 eV are shown by vertical bars in Fig. 1(b). The lower black bars mark thresholds for direct K-shell ionization of ground-level C^{2+} ions. The upper blue bars mark thresholds for direct K-shell ionization of the metastable $C^{2+}(1s^22s2p\ {}^3P)$ ions.

The HFR calculations and the measurements show two pronounced steps in the double-ionization cross-section function. The dominant step observed in the experiment at about 340 eV is obviously related to the removal of a $1s$ electron from an initial ground-level C^{2+} ion producing the $1s2s^2\ {}^2S$ level. The associated step in the HFR cross section originating from ground-level C^{2+} occurs at about 342.5 eV. The deviation from the experimental energy is not untypical for such calculations on the HFR level.

A smaller step in the HFR cross section occurs slightly above 335 eV. It is related to the metastable $C^{2+}(^3P)$ parent-ion levels and is in good agreement with the experimental findings with respect to both the threshold energy and the height of the step. A comparison with the expected threshold energies suggests that the step at 335.5 eV is associated with intermediate $1s2s2p\ {}^4P$ levels. The barely visible step feature at about 341.4 eV is related to $1s[2s2p\ {}^3P]\ {}^2P$ levels. The experimental cross-section function is inconclusive with respect to thresholds at higher energies. Obviously, the cross sections for K-shell processes leading to such higher threshold energies are relatively small.

It is interesting to note the low plateau in the net-double-ionization cross section at energies between approximately 333.5 and 335.5 eV. The onset of the plateau is, to some extent, obscured by a resonance feature at 333.4 eV but obviously appears just above the threshold for transitions $1s^22s2p \rightarrow 1s2s^2$, where a K-shell electron is removed and the $2p$ electron simultaneously relaxes to the $2s$ subshell. In other words, the excitation energy available in the metastable $C^{2+}(1s^22s2p\ {}^3P)$ helps an incoming energy-lacking photon to overcome the barrier for direct single ionization of a $1s$ electron. One might also describe such a process as an ionization with simultaneous shakedown of an excited electron. The cross-section function for such a process might be expected to have a slow onset because the shake concept requires fast removal of the inner-shell electron, which cannot really

happen at photon energies close to the ionization threshold. We are not aware of a previous experimental observation of such a two-electron process which requires an excited parent atom or ion for the photoionization to be investigated. On the other hand, the related process of ionization accompanied by shake-up or shake-off has been well established for many years [26,27]. The term shakedown was used previously by Read [28] to describe phenomena of electron scattering from atoms at energies near autoionizing states. The only connection with the process discussed here is the exchange of energy between electrons, in the present case between the $1s$ photoelectron and the excited $2p$ electron. Shakedown has also been observed and thoroughly studied by core-photoelectron spectroscopy of laser-excited sodium [29]. In that case, the ejected photoelectron gained additional kinetic energy from the shakedown of the excited $3p$ valence electron back to the $3s$ subshell.

Another possible explanation for the plateau in the net-double-ionization cross section between 333.5 and 335.5 eV could be an unresolved Rydberg series converging to the threshold at 335.48 eV for populating $1s[2s2p\ ^3P]\ ^4P$ levels by direct ionization of metastable parent C^{2+} ions. In this case, however, the observed plateau should converge to the height of the associated direct-ionization edge, which is not the case. Further investigation of the feature observed here with better statistics and better energy resolution is desirable to clarify the origin of what might be a new many-electron effect in the photoionization of electronically excited ions.

B. Cross section for photoabsorption

Previous R-matrix calculations by Hasoğlu *et al.* for the C^{2+} ion [2] provided the energy-dependent photoabsorption cross section σ_{absorb}. Absorption by C^{2+} of a photon with an energy well below 500 eV can lead to C^{q+} product ions only in final charge states $q = 2$, 3, or 4 (see also the discussion in Sec. IV A). Hence, in the present energy range, the total absorption cross section of the C^{2+} ion is the sum of partial cross sections σ_{2q} for net $(q-2)$-fold ionization of the initial C^{2+} ion with $q = 2, 3, 4$, i.e., $\sigma_{\text{absorb}} = \sigma_{23} + \sigma_{24} + \sigma_{22}$. In other words, photoabsorption in this case comprises the partial cross sections σ_{23} for net single ionization and σ_{24} for net double ionization as well as σ_{22} for K-shell excitation of the C^{2+} ion with subsequent stabilization of the charge state $q = 2$ by photoemission. As discussed above, the latter contribution is very small. The probability for Auger decay of a K vacancy is much higher than the probability for radiative decay. Therefore, the sum of the measured cross sections from Figs. 1(a) and 1(b) must be expected to be very close to the photoabsorption cross section, and thus, a meaningful comparison with the results of the R-matrix calculations is possible. One has to keep in mind, however, that the experimental result is obtained for a mixture of C^{2+} ions in the $1s^22s^2\ ^1S$ ground level and the $1s^22s2p\ ^3P$ metastable levels. Moreover, the experimental energy spread has to be considered. To model the experimental cross section on the basis of theory, the weighted sum of 68% ground-state contributions and 32% metastable contributions

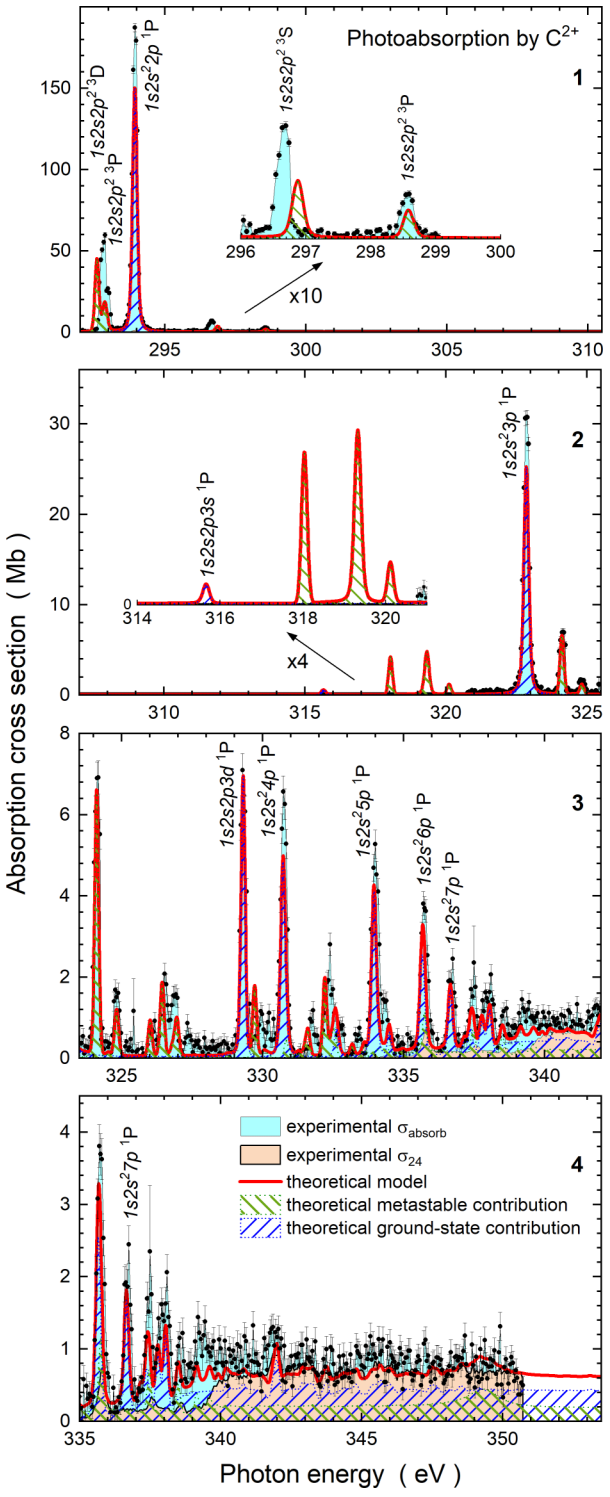

FIG. 2. Experimental cross-section function (cyan shading) for photoabsorption by C^{2+} ions compared with a theoretical model (solid red line; see text). The measured contribution of net double ionization to the photoabsorption is shown by a black solid line with light-orange shading. The theoretical contributions of ground-level ions (dotted blue line with blue upward hatching) and metastable ions (dashed green line with green downward hatching) are also displayed.

was convoluted with a Gaussian distribution of 160 meV FWHM. Figure 2 shows the *R*-matrix model calculations (the solid red line) in comparison with the experimental results.

The theoretical curves are shifted by 0.386 eV towards higher energies so that the measured position of the $1s2s^22p\ ^1P$ resonance is matched by theory. The panels each cover a photon-energy range $\Delta E = 18.5$ eV. The energy ranges overlap with one another to facilitate orientation within the spectrum. The cross-section axes vary considerably due to the decreasing sizes of the resonances, which are approximately between 0.2 and 200 Mb. The cyan shading under the experimental cross-section function indicates the contribution of net single ionization to photoabsorption; the light-orange shading is used for the contribution of net double ionization.

Panel 1 shows the resonances associated with $1s \rightarrow 2p$ excitations in both metastable- and ground-level ions. The dominant peak in the spectrum is associated with the excitation $1s^22s^2\ ^1S \rightarrow 1s2s^22p\ ^1P$. The calculated contribution arising from ground-level C^{2+} ions is represented by a blue dotted line with blue upward hatching. All other peaks arise from photoexcitation of ^3P metastable C^{2+} ions. The calculated contributions arising from metastable parent C^{2+} ions are represented by a green dashed line with green downward hatching. Identifications of the observed resonances are provided. They are based on the previous photoionization work on C^{2+} [2,7] and on separate calculations using the Cowan code [20]. The ^3P resonance at about 292.97 eV is associated with the *K*-shell excited $[1s2s\ ^1S]2p^2\ ^3P$ level, and the ^3P resonance at about 298.59 eV is associated with the *K*-shell excited $[1s2s\ ^3S]2p^2\ ^3P$ level. In the inset of panel 1 the energy range from 296 to 300 eV is expanded, and the cross section is multiplied by a factor of 10 to show the small resonances more clearly.

Panel 2 is dominated by the $1s2s^23p\ ^1P$ resonance populated from the C^{2+} ground state. The experiment missed the resonances predicted by theory in the energy range from 315 to 320.5 eV; that is, unfortunately, no measurements were performed in that energy range. The resonance contributions from metastable parent ions in this panel and in the following panels could not be unambiguously assigned. The color coding of the different lines and hatching patterns is the same in all panels.

In panel 3, the high end of a Rydberg sequence can be seen, which is associated with transitions $1s^22s^2\ ^1S \rightarrow 1s2s^2np\ ^1P$ with $n = 4, 5, 6, 7$. Higher members of the series are blended with other features of the spectrum and cannot be identified. It is interesting to note the relatively prominent occurrence of a resonance at 329.32 eV that is attributed to the excitation $1s^22s^2\ ^1S \rightarrow 1s2s2p3d\ ^1P$. This may be interpreted as a direct-double-excitation process by absorption of a single photon. Energy-shifted (0.386 eV; see above) theory and experiment for this resonance are in excellent agreement with one another.

Panel 4 covers the energy range at and just above the thresholds for direct *K*-shell single ionization by a single photon. Structure in the cross section, particularly the contribution arising from ground-state C^{2+} ions, at energies above 340 eV must be associated with double-excitation resonances. While some of the features predicted by theory can be found in the experimental spectrum, such as the resonance at about 342 eV, the prediction of a very broad resonance in the *K*-shell excitation of metastable C^{2+} at approximately 349.5 eV appears to be an artifact of the theoretical model employed in the calculations.

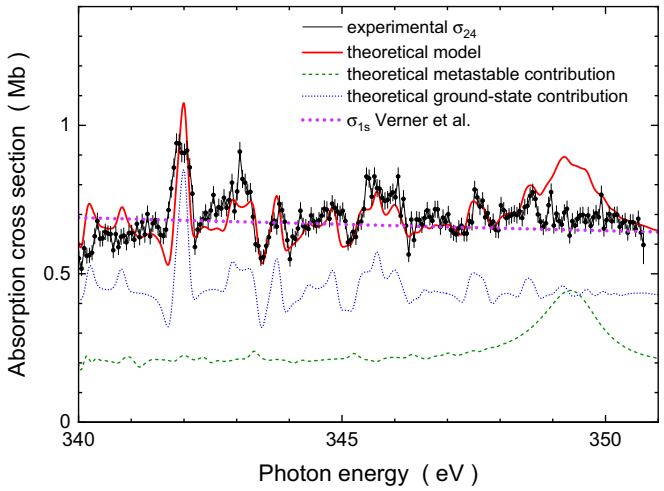

FIG. 3. Calculated and measured photoabsorption cross sections of the C^{2+} ion in the energy range from 340 to 351 eV. Instead of the sum of single and double ionization, only the measured cross section for net double ionization of the C^{2+} ion is shown. The *R*-matrix model is represented by the solid red line. The calculated contribution from ground-level ions is shown in blue, and the contribution from metastable ions is in green. The thick dots result from a calculation by Verner *et al.* [19] of the cross section σ_{1s} for direct *K*-shell ionization by a single photon.

The overall agreement of theory and experiment is very satisfying. The largest deviation in resonance energies is found for the $1s2s2p^2\ ^3S$ resonance (after correction of the theoretical energy scale by the 0.386-eV shift). It amounts to no more than 0.21 eV. Within the experimental uncertainties, theory reproduces most of the measured sizes of resonances and ionization continua. Again, the largest relative discrepancy between theory and experiment is found for the $1s2s2p^2\ ^3S$ resonance, where theory underestimates the resonance strength by roughly a factor of 2. The broad resonance predicted by theory at about 349.5 eV which is not observed in the experiment contributes only about 0.2 Mb at its maximum to the total absorption, and thus, the resulting discrepancy between the theoretical and experimental cross sections is smaller than 30%.

Figure 3 presents the comparison of theory and experiment at photon energies between 340 and 351 eV drawn on a larger scale. The energy spread in the *R*-matrix calculations is 160 meV as in Fig. 2. Rather than showing the sum of the experimental cross sections for net single and double ionization of C^{2+}, only the cross section σ_{24} for net double ionization is shown. Essentially, single ionization does not contribute to photoabsorption in the present energy range. Thus, the scatter in the photoabsorption cross section arising from the relatively bad statistics of the single-ionization measurement can be avoided. Accordingly, the statistical error bars provided in Fig. 3 are much smaller than those of the photoabsorption data displayed in panel 4 of Fig. 2. This allows for a more

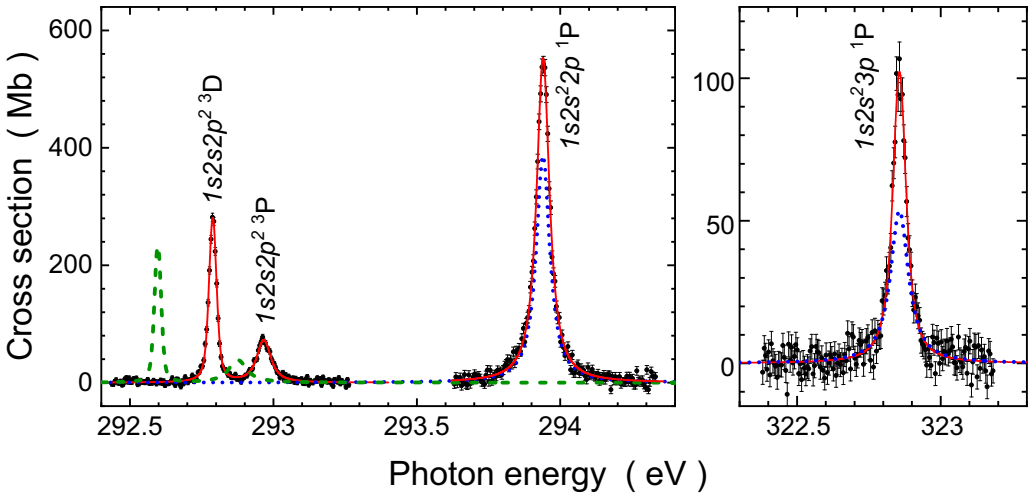

FIG. 4. Measured cross sections for net single ionization of C^{2+} ions measured at high energy resolution. The strongest resonance at about 294 eV was measured at a photon-energy bandwidth of 11 meV. All other measurements were carried out with a resolution of 22 meV. The solid red lines are fits to the spectra as described in the text. The parent ion beam contained 32% metastable ^3P and 68% ^1S ground-level ions. Accordingly, the other curves show the contributions of metastable (green dashed) and ground-state parent (blue dotted) ions as predicted by theory [2].

sensitive comparison between the experiment and the theoretical models.

The theoretical calculations by Verner *et al.* [19] describe the direct K-shell ionization of ground-state C^{2+}. This result reproduces the average of the measured cross sections very well. As mentioned above, there is the possibility for contributions from double excitation followed by emission of two electrons. The associated resonant channels can be expected to interfere with direct K-shell ionization followed by Auger emission. Thus, Fano profiles for double-excitation resonances are likely, as the R-matrix calculations demonstrate. Most of the structure arises from ground-state C^{2+}, and remarkable agreement between theory and experiment is found within the limitations of the statistical precision of the measurements. As already mentioned, the broad resonance feature predicted at 349.5 eV for photoabsorption by metastable excited C^{2+} could not be unambiguously identified in the experimental absorption cross section and was not found in the measured cross section σ_{24} for net double ionization either, while all the major double-excitation resonances originating from the ground level of C^{2+} were observed in the double-ionization channel. Therefore, we suggest that the calculated broad 249.5-eV resonance is not real.

C. High-resolution measurements and linewidths

Some of the strongest single-ionization resonances were remeasured with a substantially increased energy resolution. The resulting narrow-range spectra are displayed in Fig. 4. The measured resonances in the left panel were investigated previously [7] at an energy resolution of 68 meV. Voigt-profile fits of the ^3D and ^3P pair of resonances in the present high-resolution measurement provided a Gaussian width of 22.4 ± 1.2 meV. For the strong, separately measured $1s2s^22p\ ^1P$ resonance a Gaussian width of 11.0 ± 5.5 meV was found. The previous measurement of the $1s2s^23p\ ^1P$ resonance was carried out at a resolution of 200 meV, while a Voigt fit of the present high-resolution measurement yields a resolution of 22.0 ± 7.8 meV.

From the Voigt fits, Lorentzian widths of the four resonances shown in Fig. 4 were found to be 15.2 ± 1.1, 49.5 ± 2.4, 51.9 ± 1.5, and 46.5 ± 4.8 meV in the sequence of increasing resonance energies. The first two of these results do not have the meaning of the natural widths of the associated resonances since they comprise three individual unresolved levels each, $^3D_{1,2,3}$ and $^3P_{0,1,2}$, respectively. The remaining ^1P resonances were measured with an energy spread much smaller than their natural linewidths. Accordingly, the blue dotted lines in the two panels show the natural profiles of the calculated $1s2s^22p\ ^1P$ and $1s2s^23p\ ^1P$ resonance contributions. To obtain the green dotted line in the left panel of Fig. 4, the theoretical model cross sections were convoluted with Gaussians of 22 meV FWHM. As before, the theoretical energy scale was shifted upwards by 0.386 eV. At the present level of resolution, discrepancies between theoretical and experimental line positions are particularly emphasized. It is all the more remarkable that the resonance positions of the ^1P resonances on the shifted R-matrix energy scale perfectly line up with the experiment. Similarly, good agreement of theoretical and experimental $1s2s^2np\ ^1P$ resonances was already observed in the context of Fig. 3.

V. SUMMARY

Net single and double photoionization cross sections for the C^{2+} ion were measured. The experiments greatly extend the energy range of previous measurements on C^{2+}. The much improved capability to investigate processes with small cross sections facilitated the double-ionization measurements. Moreover, the most important resonances could be measured at a photon-energy resolution that was up to a factor of 6 better than that of the previous C^{2+} K-shell-excitation experiments.

From the measured data, photoabsorption cross sections were derived. The results are in very satisfying

agreement with previous *R*-matrix calculations. Benchmarking such calculations is important for their applications in the interpretation of astrophysical observations.

The experiment suggests the presence of an interesting multielectron process in which an excited electron in the parent ion is shaken down in a *K*-shell photoionization process that thereby boosts the insufficient energy of the incoming photon, allowing it to overcome the ionization threshold.

An important next step in the quest to better understand photoprocesses of ions is the extension of experiments to still higher photon energies where more than one inner-shell electron can be involved in the photoabsorption process and more than two electrons can be released from the parent ion. For example, signatures of direct double ionization of the *K* shell by a single photon have been seen in the net fivefold ionization of carbon anions [12]. Quantifying the contributions of direct two-electron processes to photoabsorption by ions is difficult because of the low cross sections involved. Nevertheless, further experiments should be attempted to elucidate the field of multielectron processes in single-photon absorption by (carbon) ions.

ACKNOWLEDGMENTS

This research was carried out in part at the light source PETRA III at DESY, a member of the Helmholtz Association (HGF). We gratefully acknowledge support from Bundesministerium für Bildung und Forschung provided within the "Verbundforschung" funding scheme (Contracts No. 05K19GU3 and No. 05K19RG3). We are grateful for the contributions of J. Hellhund and the late A. L. D. Kilcoyne to the measurements reported here. We gratefully acknowledge the outstanding contributions of the late S. Ricz to the realization of the experimental setup and to the data collection for the present publication. We thank the P04 beamline team for their support of our work. We are grateful to M. F. Hasoğlu and collaborators for providing their numerical *R*-matrix data. M.M. acknowledges financial support by Deutsche Forschungsgemeinschaft SFB925/A3 via Grant No. 201267377.

[1] M. Asplund, N. Grevesse, A. J. Sauval, and P. Scott, The chemical composition of the sun, Annu. Rev. Astron. Astrophys. **47**, 481 (2009).

[2] M. F. Hasoğlu, S. A. Abdel-Naby, T. W. Gorczyca, J. J. Drake, and B. M. McLaughlin, K-shell photoabsorption studies of the carbon isonuclear sequence, Astrophys. J. **724**, 1296 (2010).

[3] S. Dörner, L. Schwob, K. Atak, K. Schubert, R. Boll, T. Schlathölter, M. Timm, C. Bülow, V. Zamudio-Bayer, B. von Issendorff, J. T. Lau, S. Techert, and S. Bari, Probing structural information of gas-phase peptides by near-edge x-ray absorption mass spectrometry, J. Am. Soc. Mass Spectrom. **32**, 670 (2021).

[4] A. S. Schlachter, M. M. Sant'Anna, A. M. Covington, A. Aguilar, M. F. Gharaibeh, E. D. Emmons, S. W. J. Scully, R. A. Phaneuf, G. Hinojosa, I. Álvarez, C. Cisneros, A. Müller, and B. M. McLaughlin, Lifetime of a K-shell vacancy in atomic carbon created by $1s \rightarrow 2p$ photoexcitation of C^+, J. Phys. B **37**, L103 (2004).

[5] A. Müller, A. Borovik, Jr., T. Buhr, J. Hellhund, K. Holste, A. L. D. Kilcoyne, S. Klumpp, M. Martins, S. Ricz, J. Viefhaus, and S. Schippers, Observation of a Four-Electron Auger Process in Near-*K*-Edge Photoionization of Singly Charged Carbon Ions, Phys. Rev. Lett. **114**, 013002 (2015).

[6] A. Müller, A. Borovik, Jr., T. Buhr, J. Hellhund, K. Holste, A. L. D. Kilcoyne, S. Klumpp, M. Martins, S. Ricz, J. Viefhaus, and S. Schippers, Near-*K*-edge single, double, and triple photoionization of C^+ ions, Phys. Rev. A **97**, 013409 (2018).

[7] S. W. J. Scully, A. Aguilar, E. D. Emmons, R. A. Phaneuf, M. Halka, D. Leitner, J. C. Levin, M. S. Lubell, R. Püttner, A. S. Schlachter, A. M. Covington, S. Schippers, A. Müller, and B. M. McLaughlin, K-shell photoionization of Be-like carbon ions: Experiment and theory for C^{2+}, J. Phys. B **38**, 1967 (2005).

[8] A. Müller, S. Schippers, R. A. Phaneuf, S. W. J. Scully, A. Aguilar, A. M. Covington, I. Álvarez, C. Cisneros, E. D. Emmons, M. F. Gharaibeh, G. Hinojosa, A. S. Schlachter, and B. M. McLaughlin, K-shell photoionization of ground-state Li-like carbon ions [C^{3+}]: Experiment, theory and comparison with time-reversed photorecombination, J. Phys. B **42**, 235602 (2009).

[9] A. Müller, E. Lindroth, S. Bari, A. Borovik, Jr., P.-M. Hillenbrand, K. Holste, P. Indelicato, A. L. D. Kilcoyne, S. Klumpp, M. Martins, J. Viefhaus, P. Wilhelm, and S. Schippers, Photoionization of metastable heliumlike $C^{4+}(1s2s\ ^3S_1)$ ions: Precision study of intermediate doubly excited states, Phys. Rev. A **98**, 033416 (2018).

[10] N. D. Gibson, C. W. Walter, O. Zatsarinny, T. W. Gorczyca, G. D. Ackerman, J. D. Bozek, M. Martins, B. M. McLaughlin, and N. Berrah, K-shell photodetachment from C^-: Experiment and theory, Phys. Rev. A **67**, 030703(R) (2003).

[11] C. W. Walter, N. D. Gibson, R. C. Bilodeau, N. Berrah, J. D. Bozek, G. D. Ackerman, and A. Aguilar, Shape resonance in K-shell photodetachment from C^-, Phys. Rev. A **73**, 062702 (2006).

[12] A. Perry-Sassmannshausen, T. Buhr, A. Borovik, Jr., M. Martins, S. Reinwardt, S. Ricz, S. O. Stock, F. Trinter, A. Müller, S. Fritzsche, and S. Schippers, Multiple Photodetachment of Carbon Anions via Single and Double Core-Hole Creation, Phys. Rev. Lett. **124**, 083203 (2020).

[13] A. Müller, Precision studies of deep-inner-shell photoabsorption by atomic ions, Phys. Scr. **90**, 054004 (2015).

[14] A. Müller, R. A. Phaneuf, A. Aguilar, M. F. Gharaibeh, A. S. Schlachter, I. Alvarez, C. Cisneros, G. Hinojosa, and B. M. McLaughlin, Photoionization of C^{2+} ions: Time-reversed recombination of C^{3+} with electrons, J. Phys. B **35**, L137 (2002).

[15] A. Müller, S. Schippers, R. A. Phaneuf, A. L. D. Kilcoyne, H. Bräuning, A. S. Schlachter, M. Lu, and B. M. McLaughlin, State-resolved valence shell photoionization of Be-like ions: Experiment and theory, J. Phys. B **43**, 225201 (2010).

[16] S. Schippers *et al.*, Absolute cross sections for photoionization of Xe^{q+} ions ($1 \leqslant q \leqslant 5$) at the 3d ionization threshold, J. Phys. B **47**, 115602 (2014).

[17] A. Müller, D. Bernhardt, A. Borovik, Jr., T. Buhr, J. Hellhund, K. Holste, A. L. D. Kilcoyne, S. Klumpp, M. Martins, S. Ricz, J. Seltmann, J. Viefhaus, and S. Schippers, Photoionization of Ne atoms and Ne^+ ions near the K edge: Precision spectroscopy and absolute cross-sections, Astrophys. J. **836**, 166 (2017).

[18] J. Viefhaus, F. Scholz, S. Deinert, L. Glaser, M. Ilchen, J. Seltmann, P. Walter, and F. Siewert, The variable polarization XUV beamline P04 at PETRA III: Optics, mechanics and their performance, Nucl. Instrum. Methods Phys. Res. Sect. A **710**, 151 (2013).

[19] D. A. Verner, G. F. Verland, K. T. Korista, and D. G. Yakovlev, Atomic data for astrophysics. II. New analytic fits for photoionization cross sections of atoms and ions, Astrophys. J. **465**, 487 (1996).

[20] R. D. Cowan, *The Theory of Atomic Structure and Spectra* (University of California Press, Berkeley, 1981)

[21] M. Martins, Photoionization of open-shell atoms: The chlorine 2p excitation, J. Phys. B **34**, 1321 (2001).

[22] F. F. Goryaev, L. A. Vainshtein, and A. M. Urnov, Atomic data for doubly-excited states $2lnl'$ of He-like ions and $1s2lnl'$ of Li-like ions with Z = 6-36 and n = 2, 3, At. Data Nucl. Data Tables **113**, 117 (2017).

[23] A. E. Kramida, Yu. Ralchenko, J. Reader, and NIST ASD Team, NIST Atomic Spectra Database, version 5.10, https://physics.nist.gov/asd.

[24] V. A. Yerokhin, A. Surzhykov, and A. Müller, Relativistic configuration-interaction calculations of the energy levels of the $1s^22l$ and $1s2l2l'$ states in lithiumlike ions: Carbon through chlorine, Phys. Rev. A **96**, 042505 (2017).

[25] V. A. Yerokhin, A. Surzhykov, and A. Müller, Erratum: Relativistic configuration-interaction calculations of the energy levels of the $1s^22l$ and $1s2l2l'$ states in lithiumlike ions: Carbon through chlorine [Phys. Rev. A **96**, 042505 (2017)], Phys. Rev. A **96**, 069901(E) (2017).

[26] T. A. Carlson and M. O. Krause, Experimental Evidence for Double Electron Emission in an Auger Process, Phys. Rev. Lett. **14**, 390 (1965).

[27] A. Kheifets, Shake-off process in non-sequential single-photon double ionization of closed-shell atomic targets, Atoms **10**, 89 (2022).

[28] F. H. Read, Displaced electron energies and the "shake-down" effect, Radiat. Res. **64**, 23 (1975).

[29] J. Schulz, M. Tchaplyguine, T. Rander, O. Björneholm, S. Svensson, R. Sankari, S. Heinäsmäki, H. Aksela, S. Aksela, and E. Kukk, Shakedown in core photoelectron spectra from aligned laser-excited Na atoms, Phys. Rev. A **72**, 010702(R) (2005).